Anchoring Subnanometric Cu_4 Clusters in Graphitic-C_3N_5 for Highly Efficient CO_2 Photoreduction to Ethanol

Entian Cui,[a] Yulian Lu,[a] Xiu-Li Yang,[a,*] Guojun Dong,[b] Yajun Zhang,[b] Yingpu Bi[b*]

[a] Key Laboratory for Advanced Technology in Environmental Protection of Jiangsu Province, Yancheng Institute of Technology, Yancheng 224051 (P. R. China)

[b] State Key Laboratory for Oxo Synthesis & Selective Oxidation, National Engineering Research Center for Fine Petrochemical Intermediates, Lanzhou Institute of Chemical Physics, CAS Lanzhou 730000 (P. R. China)

* E-mail: xlyang@ycit.edu.cn; yingpubi@licp.cas.cn

Materials and Methods

Chemical reagents. Melamine (99%), hydrazine hydrate (55%), HCl (37%), copper dinitrate ($Cu(NO_3)_2$), ethanol (C_2H_5OH), Nafion solution (5wt%), potassium hydroxide (KOH), Sodium sulfate anhydrous (Na_2SO_4), potassium nitrate (KNO_3), and ethanol (99.8%) were obtained from Shanghai Macklin Biochemical Technology Co., Ltd. All chemicals were used without any additional purification. The water used in all experiments with a resistivity of 18.2 MΩ was prepared using an ultrapure water system.

Characterizations. The phase structures of as-prepared samples were identified by the Rigaku B/Max-RB X-ray diffractometer. The morphologies and microstructures of the prepared samples were observed by field emission transmission electron microscopy (TEM, JEOL JEM-2100F) and high-solution TEM (HRTEM) operated at 200 kV. The surface electronic states and element composition were determined by X-ray photoelectron spectroscopy (XPS, ESCALAB 250Xi). UV-vis diffuse reflectance spectra were tested on a UV-2550 (Shimadzu) spectrophotometer. The FTIR spectra were recorded as a function of time to investigate the dynamics of the conversion of the reactants under irradiation. The desorption performances of CO_2 were characterized by a temperature programmed chemical adsorption instrument (TPD, Chemisorb 2720; Micromeritics). Photoluminescence spectra (PL) and transient absorption spectra (TAS) were recorded on an Edinburgh LP 980 spectrofluorimeter. The element molar ratios were obtained by inductively coupled plasma mass spectrometer (ICP-MS, NexION 300X). In situ DRIFTS measurements were performed on Bruker VERTEX 70 infrared instrument equipped with a tailor-made reactor and a 300 W Xenon lamp. Typically, the loaded samples were evenly placed in the bottom of the analyzed chamber and sealed. Subsequently, a mixed atmosphere (CO_2 with a trace of H_2O vapor) was introduced into the reactor for 20 min at room temperature. After reaching the sorption equilibrium, the DRIFTS spectra were acquired by the dynamics of the transition of the reactants under illumination. The Quasi in-situ X-ray photoelectron spectroscopy (QIS-XPS) instrument was equipped with a 300 W Xe lamp as light source. Before QIS-XPS measurements, after being made into thin sheets with suitable size, the photocatalyst was placed in a sealed adsorption chamber and purged with Ar (50 mL min^{-1}) at 120°C for 30 min to remove the surface adsorbed impurities. Subsequently, a CO_2/H_2O (vapor) mixed gas with 80:20 volume ratio was purged into

the chamber at room temperature for 20 min to reach the adsorption equilibrium. Finally, the as-prepared samples were quickly transferred to the analysis chamber of XPS instrument (ESCALAB 250Xi) for the QIS-XPS measurements. The variations of XPS spectra were recorded by controlling light irradiation (on or off). X-ray adsorption near edge structure (XANES) measurements were measured at Shanghai Synchrotron Radiation Facility in China. The output beam was selected by Si(111) monochromator. The data were collected at room temperature under fluorescence mode by using solid state detector.

Preparation of C_3N_5. The bulk C_3N_5 was prepared following the previous report.[1]

Preparation of Cu/C_3N_5. The melem hydrazine powder was prepared following the previous report.[1] 340 mg $Cu(NO_3)_2{\cdot}3H_2O$ was firstly dissolved in ethanol by stirring at 50°C, and then 3 g melem hydrazine powder was added into the above solution with sonication for 30 min to gain a well-dispersed suspension. The suspension was kept on stirring for 12 h and then separated by filtration with ethanol and finally dried at 60°C. The obtained product was further pyrolyzed at 450°C with the ramping rate of 5°C min^{-1} under N_2 atmosphere. Finally, the obtained power was immersed in 0.5 M H_2SO_4 at 80°C for 12 h to remove the possible metallic Cu species.

Synthesis of Cu_4/C_3N_5. The entire preparation process was carried out in a glove box to avoid the influence of O_2. The Cu_4/C_3N_5 was constructed *via* electrochemical method in a CHI 660E electrochemical workstation equipped with a sealed H-type cell segregated by nafion-117 proton exchange membrane. Ag/AgCl equipped with salt bridge and platinum foil (5*5 cm^2) were used as the reference and counter electrodes, respectively. The working electrode was prepared as following: 20 mg Cu/C_3N_5 powder was dispersed in 100 uL 5wt% Nafion and 200 uL ethanol, and then sonicated the mixture for 30 min. The well-dispersed catalyst ink was uniformly brushed on GDL substrate with an area of 2*10 cm^2, and dried at 50°C. For the electrochemical synthesis, Ar-saturated 50 mL 0.1 M KOH including 0.1 M KNO_3 was used as electrolytes. Cyclic voltammograms (CVs) was performed. The electrocatalytic synthesis were conducted at different potentials (-0.20, -0.40, -0.60, -0.80, and -1.00 V vs. RHE) for 30 min by chronoamperometric tests. The catalyst powders were collected by gently scraping the electrode surface and then

immersed into ethanol solution for 12 h to remove the Nafion component. To obtain enough catalyst powders, the above preparation processes were repeated. The as-prepared samples were stored in inert atmosphere.

Photocatalytic CO_2 reduction measurements.

100 mg of catalyst was added to 20 mL $NaHCO_3$ aqueous solution (0.1 M), sonicated for 20 min and then transferred into a tailor-made vessel and then hermetically sealed. Before illumination, high-purity CO_2 (99.999%) was continuously purged into the solution for 30 min to produce a mixture of CO_2 and H_2O vapors to replace the atmosphere in the glass vessel. The reaction temperature of the system was maintained at 25°C by circulating cooling water. A 300 W xenon lamp (Microsolar300, PerfectLight) equipped with a 420 nm cut off filter was employed as the light source. The products were analyzed using Agilent GC 6890N gas chromatograph with a flame ionization detector (FID) and thermal conductivity detector (TCD). The chromatographic columns were di-n-butyl phthalate fill column and polyethylene glycol 20000 fill column.

To investigated the effect of possible existing Nafion residues or other organic residues, a comparative blank photocatalytic evaluation experiment without CO_2 was performed in pure water following the above procedure.

Isotopic $^{13}CO_2$ experiments. ^{13}C-labeled CO_2 ($^{13}CO_2$, 99.999%) gas was used as the feed gas in the labeling experiment. 50 mg of catalyst was added to 20 mL DMF/H_2O mixture (12.5 vol% H_2O), sonicated for 10 min and then transferred into a tailor-made vessel and then hermetically sealed. Before illumination, high-purity Ar was continuously purged into the solution at 300 mL min^{-1} for 30 min to remove air and then blown with $^{13}CO_2$ gas was purged into the vessel with the inner pressure at 1.0 MPa. The reactor temperature was kept at 25°C with a cooling water circulator. A 300 W xenon lamp (Microsolar300, PerfectLight) equipped with a 420 nm cut off filter was employed as the light source. The final production was checked by GC-MS (TRACE1310-ISQ-LT). The GC-MS spectrum of ^{12}C-labeled CO_2 was obtained following the above procedure by replacing $^{13}CO_2$ with $^{12}CO_2$ gas.

Photoelectrochemical measurements. All photoelectrochemical measurements were performed

in a three-electrode configuration (CHI 660E, Shanghai, China), in which the sample photoelectrode, Pt sheet and Ag/AgCl electrode were served as the working electrode, counter electrode and reference electrode, respectively. Na_2SO_4 aqueous solution (0.2 M) was used as electrolyte. To prepare photoelectrodes, as-prepared catalyst (5 mg) was dispersed into the 1 mL mixture solution (0.75 mL H_2O and 0.25 mL isopropanol) containing 20 μL 5% Nafion under vigorous ultrasonic treatment for 60 min. And then, 50 μL of gel solution was dip-coated on FTO glass and dried at 60°C for 2 h to obtain Cu_4/C_3N_5 electrode. A 300 W Xenon lamp was worked as illumination source. Before the photocurrent measurement, the electrolyte solution was saturated with Ar atmosphere for 30 min at room temperature.

Computational method. DFT calculations were carried out based on the Cambridge Serial Total Energy Package. The exchange-correlation energy is described by the generalized gradient approximation using the Perdew-Burke-Ernzerh (PBE) of functional. The effect of the van der Waals interactions is considered by using the empirical correction scheme of Grimme's DFT-D method. A 400 eV plane-wave kinetic energy cutoff was chosen. Geometry optimization has been done with the Brillouin zone sampling limited to the gamma point. The atomic positions were fully relaxed until a maximum energy difference and residual force on atoms, respectively, converged to 10^{-5} eV and 0.03 eV $Å^{-1}$. A 15 Å vacuum layer was added to prevent the interaction.

Additional Figures and Discussions

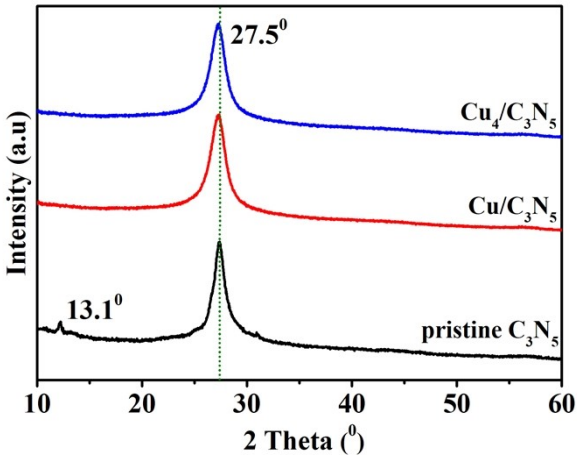

Fig. S1 XRD patterns of pristine C_3N_5, Cu/C_3N_5, and Cu_4/C_3N_5.

Additional discussions

The electrochemical treatment process did not change the structure of C_3N_5, as proved by the similar XRD patterns between pristine C_3N_5 and Cu_4/C_3N_5 (Fig. S1). The diffraction peaks at 13.1 and 27.5° could be indexed to (100) and (002) planes of graphitic-C_3N_5, respectively.[1,2] Compared to pristine C_3N_5, the (002) diffraction peaks of Cu/C_3N_5 and Cu_4/C_3N_5 shifted slightly to lower 2θ angle for the strong interaction between Cu single atoms and C_3N_5 support. However, the related anchoring of Cu single-atom or Cu_4 clusters would inevitably promote the further distortion in the graphitic-C_3N_5 framework, resulting in the disappearance (100) planes at 13.1°.

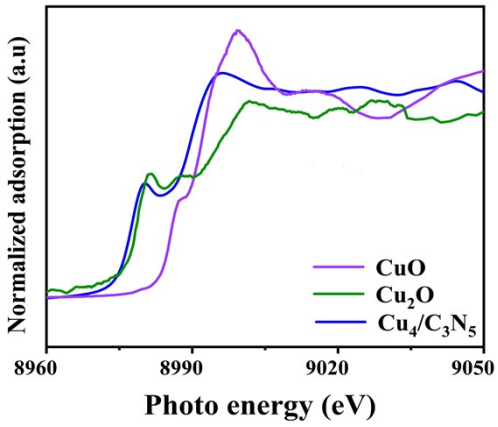

Fig. S2 Cu K-edge XANES spectra of Cu_4/C_3N_5 compared with CuO and Cu_2O.

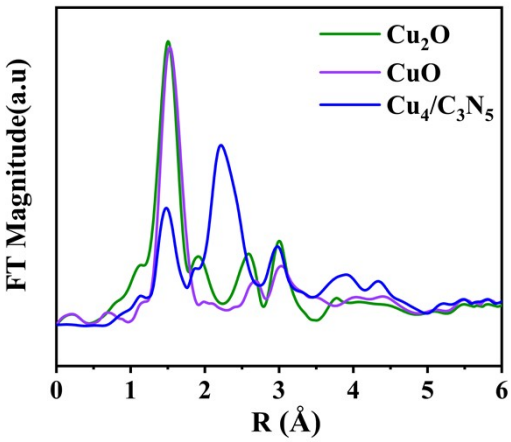

Fig. S3 R-space of EXAFS spectra of Cu_4/C_3N_5 compared with CuO and Cu_2O.

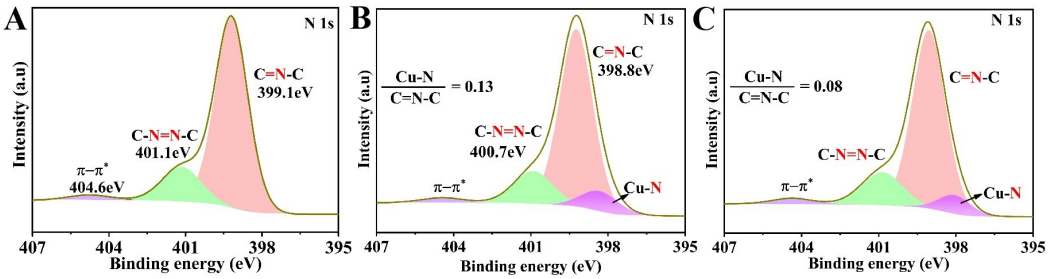

Fig. S4 The N 1s XPS of pristine C_3N_5 (A), Cu/C_3N_5 (B), and Cu_4/C_3N_5 (C).

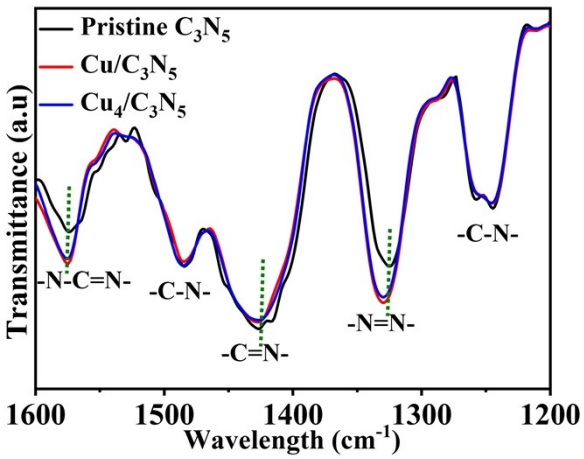

Fig. S5 The FTIR spectra of sample pristine C_3N_5, Cu/C_3N_5, and Cu_4/C_3N_5.

Additional discussions

As seen in N 1s XPS of pristine C_3N_5 (Fig. S4A), the two peaks at 399.1 and 401.1 eV were ascribed to the N atoms of secondary C=N-C and bridging C-N=N-C, respectively.[2] While in Cu_4/C_3N_5, both peaks shifted to 398.8 and 400.7 eV, respectively (Fig. S4C), suggesting the disturbed chemical- and electronic- environment of N atoms in C=N-C and C-N=N-C moiety. Furthermore, an additional deconvoluted peak at 398.6 eV appeared, which can be ascribed to Cu-N bonds.[3] The strong interaction between Cu atoms and C_3N_5 support was confirmed by the result of FTIR, in which the wavenumbers of N-C=N-, -C=N-, and -N=N- bonds in Cu_4/C_3N_5 all changed in comparison of these in pristine C_3N_5 (Fig. S5).[4] The similar changes were also detected in Cu/C_3N_5 sample.

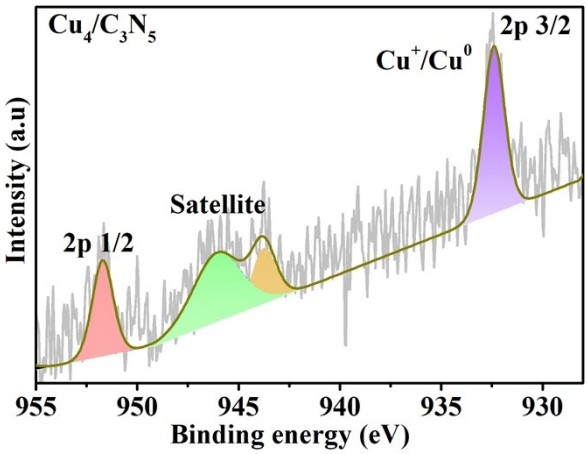

Fig. S6 The Cu 2p XPS spectrum of Cu_4/C_3N_5.

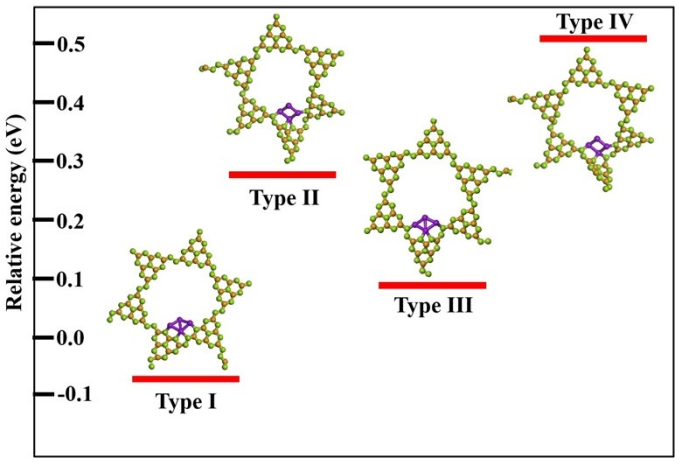

Fig. S7 Views showing the four types of Cu_4 clusters combined with C_3N_5.

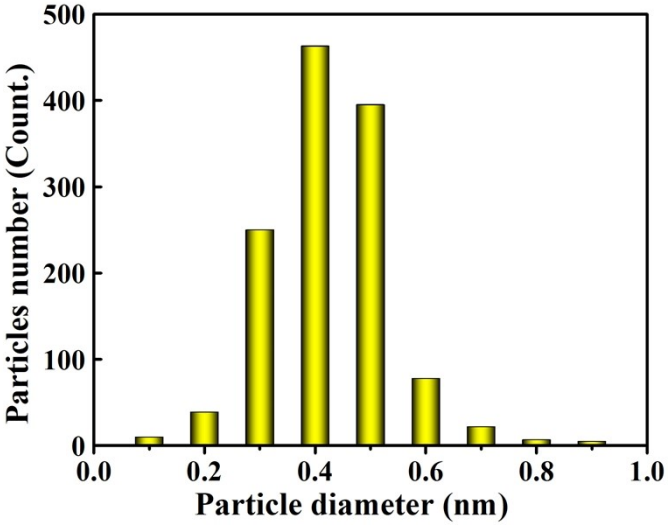

Fig. S8 The size distribution of Cu_4 clusters in Cu_4/C_3N_5.

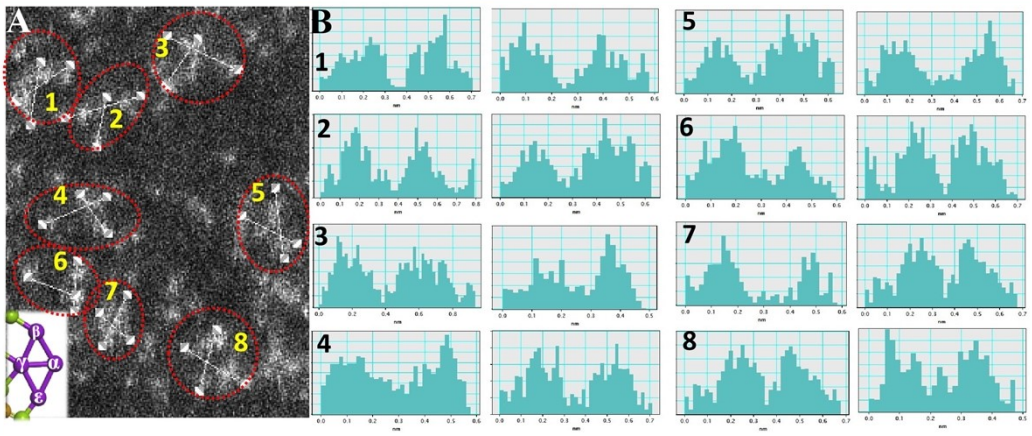

Fig. S9 (A) The aberration-corrected HAADF-STEM image of Cu_4/C_3N_5 with Cu_4 clusters marked with dashed circles. (B) The image intensity line profiles, which were taken along the solid lines in Fig. S7A.

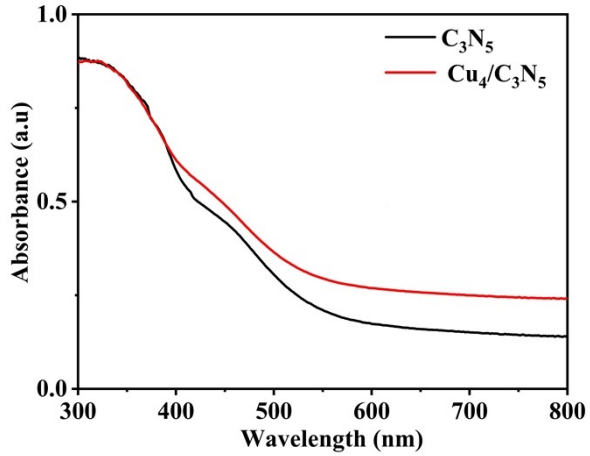

Fig. S10 UV–vis DRS of Cu_4/C_3N_5.

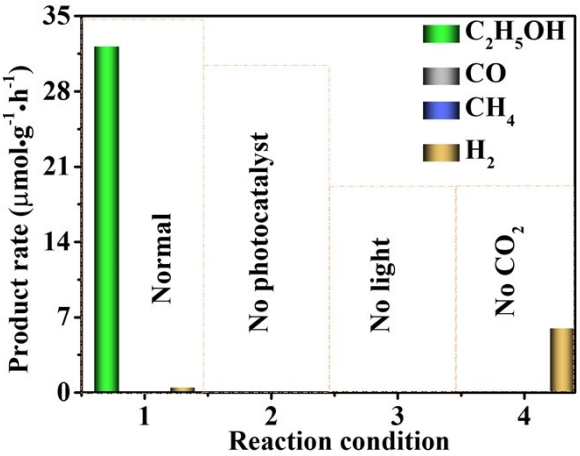

Fig. S11 CO_2 photoreduction results on Cu_4/C_3N_5 with different control conditions.

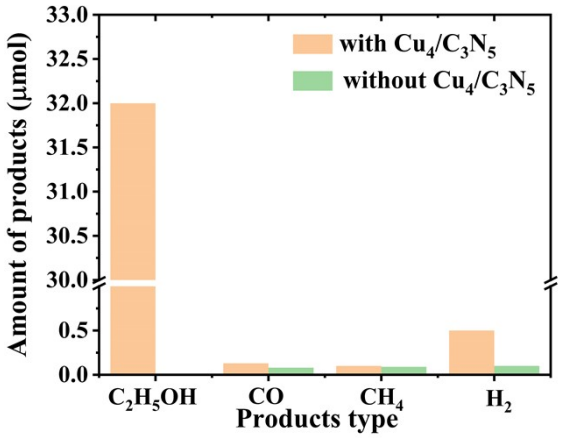

Fig. S12 The comparative photocatalytic experiment results with and without Cu_4/C_3N_5 addition

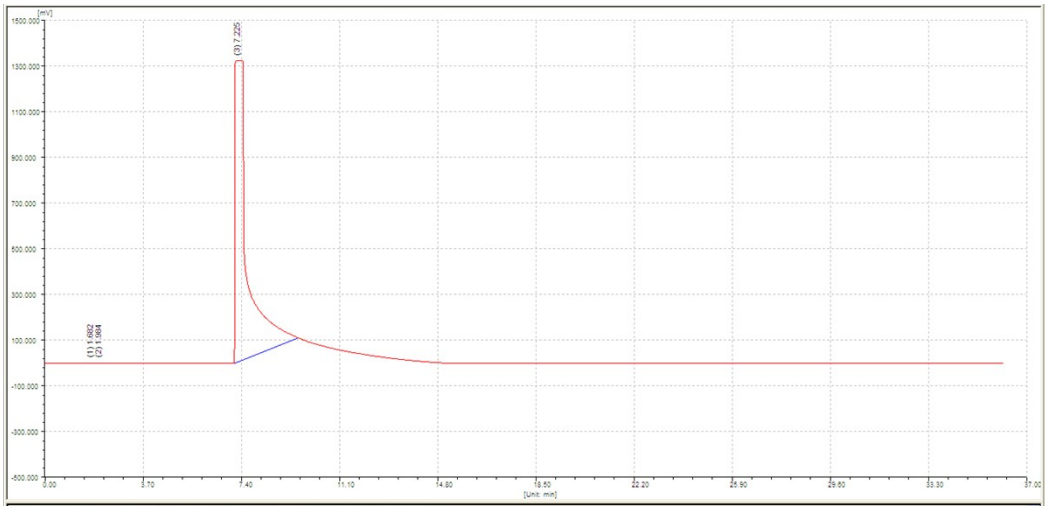

Fig. S13 The GC test result of Cu_4/C_3N_5 with light and CO_2 (FID detector).

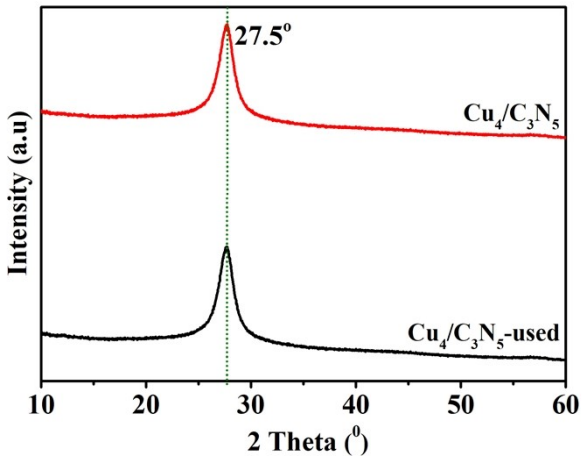

Fig. S14 The XRD patterns of Cu_4/C_3N_5 before and after photoreaction.

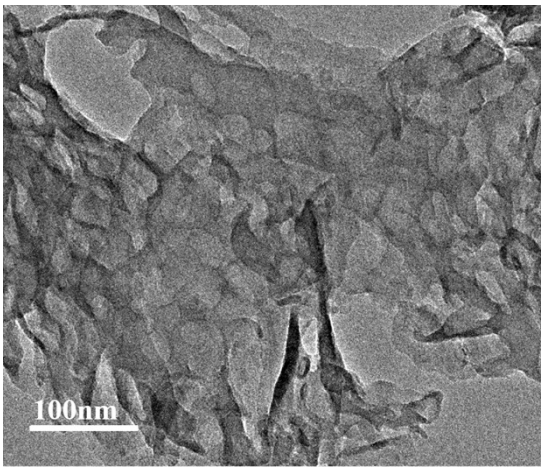

Fig. S15 The TEM image of Cu_4/C_3N_5 after photoreaction.

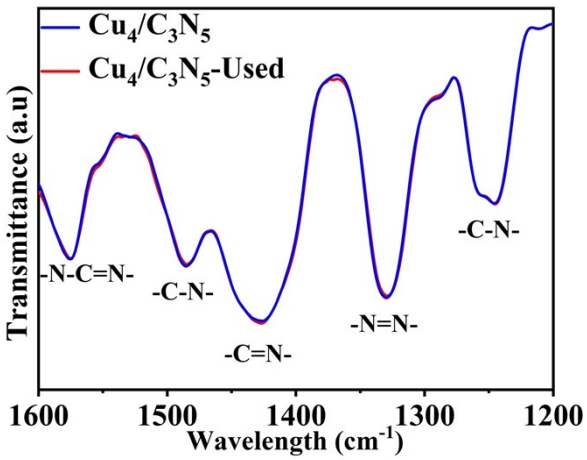

Fig. S16 The FTIR spectra of Cu_4/C_3N_5 before and after photoreaction.

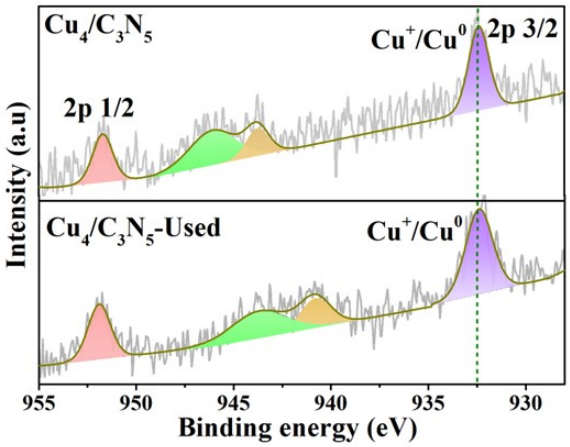

Fig. S17 The Cu 2p XPS spectra of Cu_4/C_3N_5 before and after photoreaction.

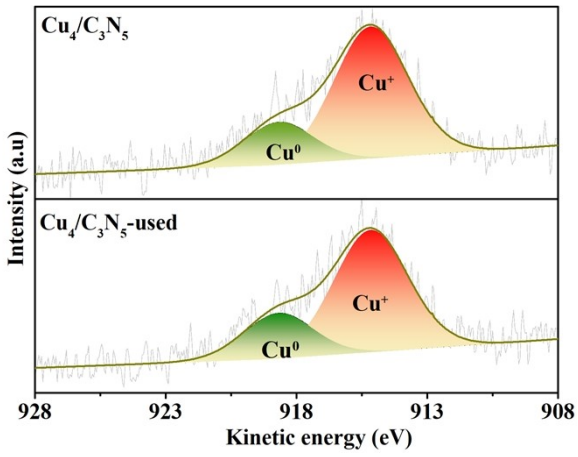

Fig. S18 The Cu LLM spectra of Cu_4/C_3N_5 before and after photoreaction.

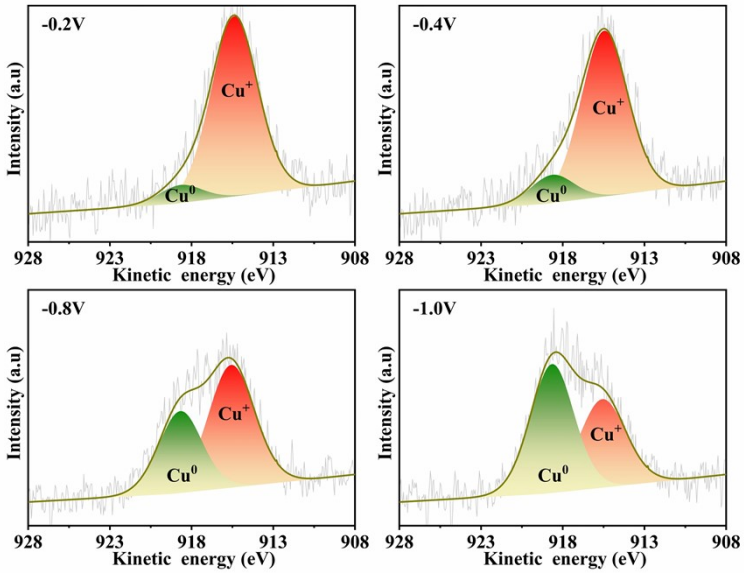

Fig. S19 Cu LLM Auger spectra of the samples obtained under different applied bias.

Additional discussions

The Cu^+/Cu^0 ratio was potential-dependent. The calculated Cu^+/Cu^0 ratios were 11.12, 6.03, 1.53, and 0.73 for the samples obtained at applied potential of -0.2, -0.4, -0.8, and -1.0 V vs RHE, respectively (Fig. S19).[5]

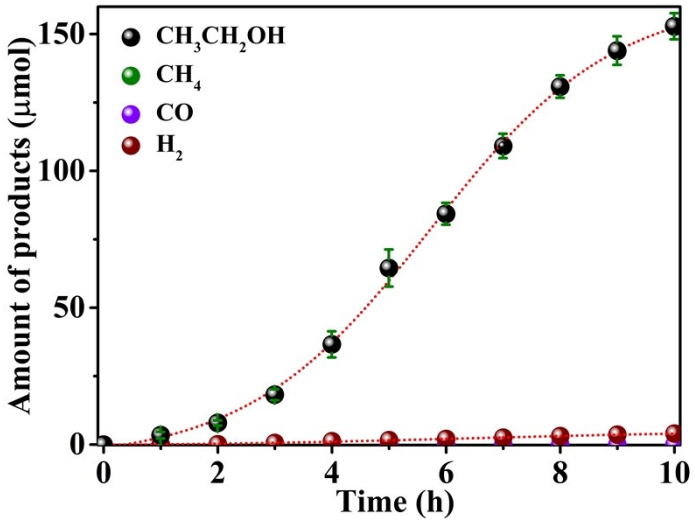

Fig. S20 Time course of CO_2 amount on Cu_4/C_3N_5 with the TEOA addition.

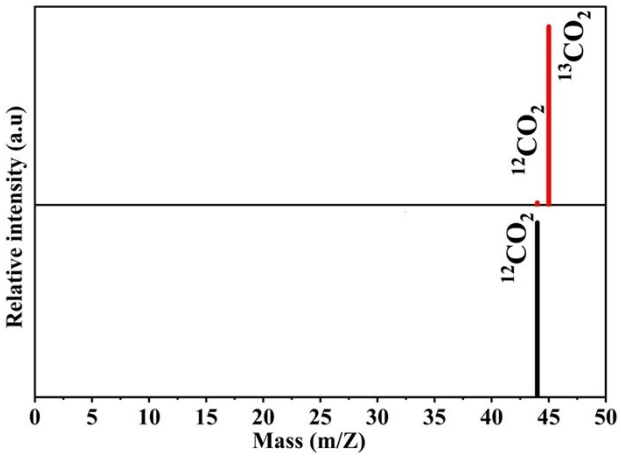

Fig. S21 MS spectra of $^{13}CO_2$ and $^{12}CO_2$.

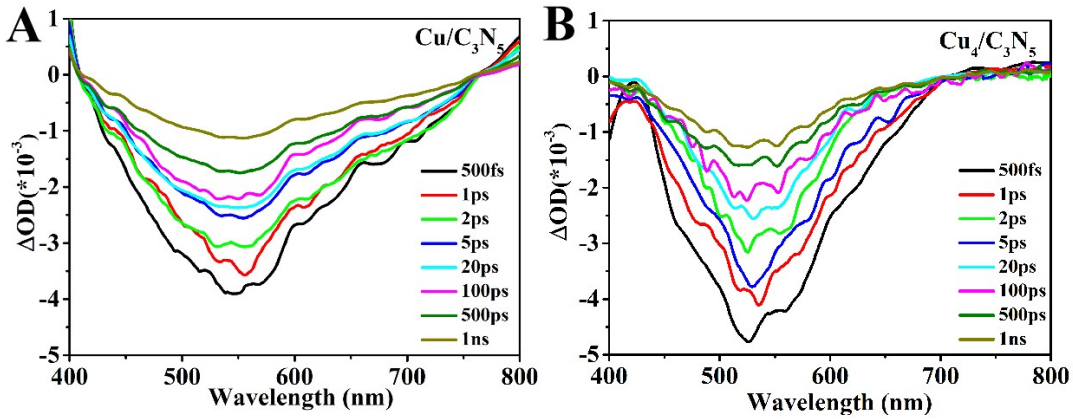

Fig. S22 Femtosecond pump-probe transient absorption spectra of Cu_4/C_3N_5 (A) and Cu/C_3N_5 (B) systems.

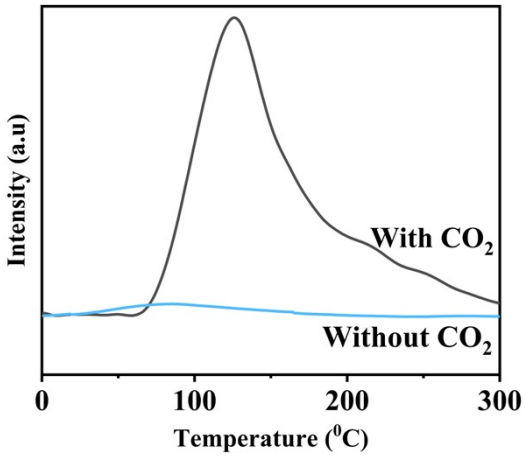

Fig. S23 TPD curves of Cu_4/C_3N_5 with and without CO_2 gas.

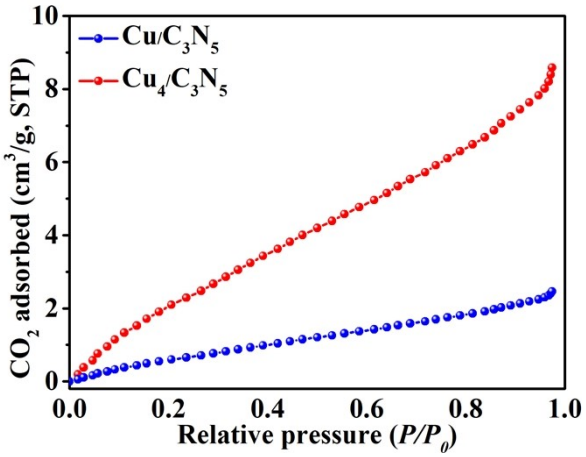

Fig. S24 CO_2 adsorption isotherm curves of Cu/C_3N_5 and Cu_4/C_3N_5.

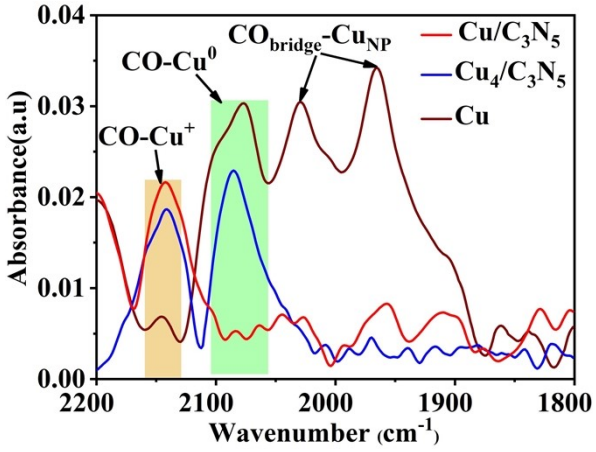

Fig. S25 The CO adsorption curves on Cu/C_3N_5 and Cu_4/C_3N_5.

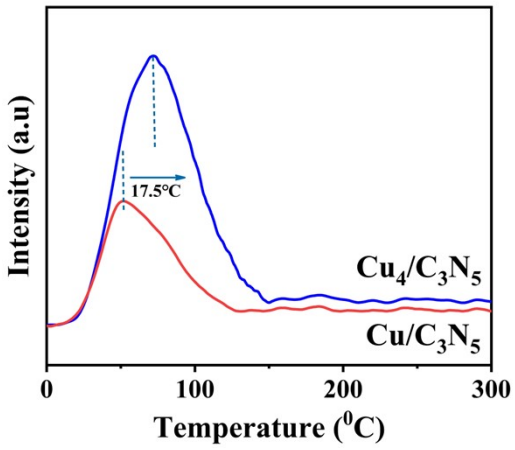

Fig. S26 CO-TPD spectra of Cu/C_3N_5 and Cu_4/C_3N_5.

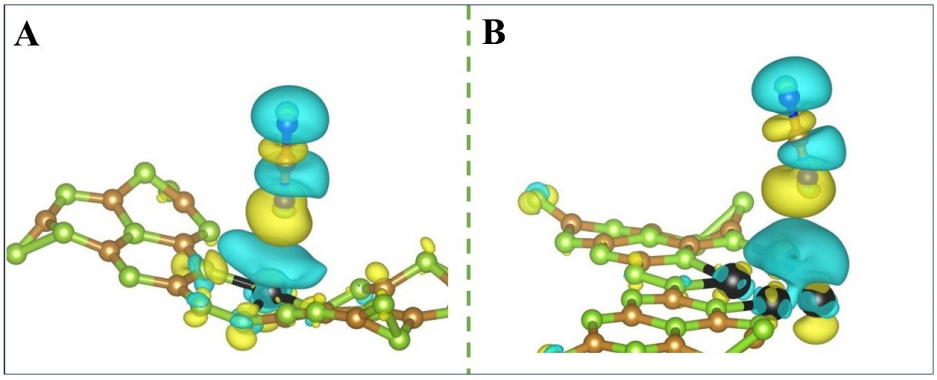

Fig. S27 Differential charge density calculations for Cu/C_3N_5 (A) and Cu_4/C_3N_5 (B) with CO_2 adsorption.

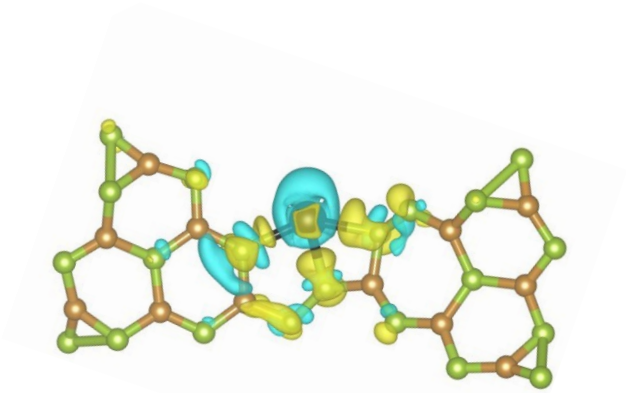

Fig. S28 Differential charge density calculations for $Cu^{\delta+}$ over Cu/C_3N_5.

Additional discussions

The charge concentration of Cu^+ atom was further reduced owing to the coordinated N atoms. Because of the asymmetrical electronic structure of Cu_4 clusters, when CO_2 adsorption, the electrons flowed from Cu atoms to adsorbed CO_2 molecules (Fig. S27), resulting in the higher CO_2 adsorption energy of Cu_4/C_3N_5 than Cu/C_3N_5 (without asymmetrical electronic structure, Fig. S28). It was beneficial for the activation of CO_2.

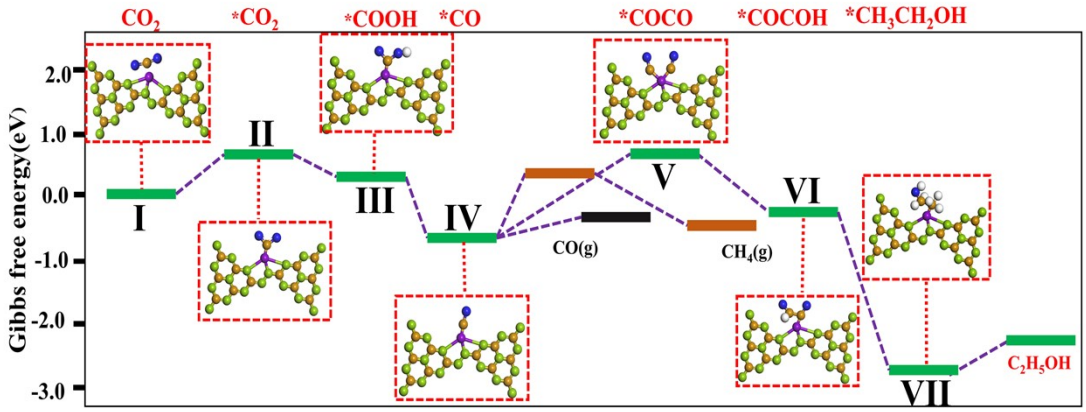

Fig. S29 Gibbs free energy diagrams and CO_2 to ethanol photoreduction pathways on Cu/C_3N_5.

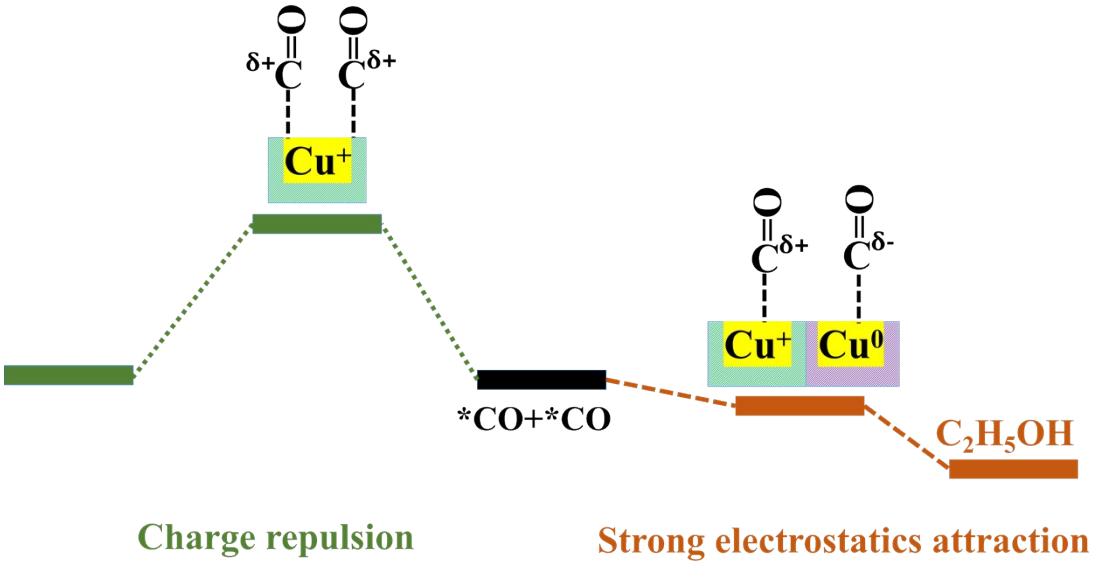

Fig. S30 Free-energy profiles for *CO dimerization on Cu/C_3N_5 and Cu_4/C_3N_5.

Additional Tables

Table S1 Structural parameters obtained from Cu K-edge EXAFS fitting.

Sample	Coordination	CN	R(Å)	$\sigma^2\times10^{-3}$(Å^2)	ΔE_O(eV)	R-factor
Cu foil	Cu-Cu	12	2.53±0.03	9.0±1.5	2.3	0.002
Cu_2O	Cu-O	4	1.84±0.02	3.1±0.4	8.3	0.006
CuO	Cu-O	4	1.94±0.02	3.6±0.9	0.2	0.004
Cu/C_3N_5	Cu-N	3.3±0.5	1.92±0.02	7.6±1.6	2.7	0.001
Cu_4/C_3N_5	Cu-N	2.2±0.5	1.91±0.04	8.9±2.1	2.3	0.002
	Cu-Cu	2.6±0.6	2.51±0.03	9.6±1.7	2.3	0.002

CN: Coordination number.

Table S2 Comparison of photocatalytic performance in CO_2 reduction to ethanol

Photocatalyst	Metal loading (wt.%)	Light source	Medium	Rate (μmol $g^{-1}h^{-}$	Sel.(%)	Refs
Cu_4/C_3N_5	2.65	300 W Xe (λ≧420nm)	H_2O	32.2	98.6	This work
Cu_4/C_3N_5	2.65	300 W Xe (λ≧420nm)	TEOA/H_2O	152.8	97.7	This work
BP/BWO	N.R	300 W Xe	H_2O	3.8	32.2	Ref [7]
BP/BWO	N.R	300 W Xe	Benzylamine/H_2O	61.3	91.0	Ref [7]
Oxide-derived Cu/PCN	0.65	300 W Xe	TEOA/H_2O	2.8	58.0	Ref [8]
C_3N_4/UiO-66(Zr/Ce)	N.R	300 W Xe	Acetonitrile/H_2O	38.1	41.1	Ref [9]
InCu/PCN	In: 1.0; Cu: 0.5	300 W Xe	DMF/H_2O	28.5	92.4	Ref [10]
Cu/PCN	Cu: 0.5	300 W Xe	DMF/H_2O	11.8	89.6	Ref [10]
STO/Cu@Ni/TiN	N.R	300 W Xe	H_2O	21.3	79.0	Ref [11]
Bi@Bi_2MoO_6	N.R	300 W Xe (λ ≧400 nm)	$NaHCO_3$	17.93	92.0	Ref [12]
TiO_2{100}	N.R	300 W UV enhanced Xe	$NaHCO_3$	6.16	66.7	Ref [13]
Cu_{SAs}/UiO-66-NH_2	0.39%	300 W Xe	TEOA/H_2O	4.22	54.3	Ref [14]
Cu-(Ni,Zr)-UiO-66-NH	Cu: 0.2; Ni: 0.2	300 W Xe (λ≧420nm)	TEOA/H_2O	7.08	97.3%	Ref [15]

N.R: not reported.

Table S3 Exponential fitting parameters for the Fluorescence of Cu_4/C_3N_5

Samples	A_1	τ_1(ns)	A_2	τ_2(ns)	A_3	τ_3(ns)	τ_{avg}(ns)	R^2
Cu/C_3N_5	0.31	6.11	0.34	2.79	0.35	6.02	5.12	0.998
Cu_4/C_3N_5	0.34	7.13	0.26	3.11	0.40	11.18	9.05	0.998

Table S4 Exponential fitting parameters for fs-TA of Cu_4/C_3N_5

Samples	A_1	τ_1(ps)	A_2	τ_2(ps)	A_3	τ_3(ps)	τ_{avg}(ps)	R^2
Cu/C_3N_5	0.40	2.11	0.31	28.15	0.29	1249.90	314.1	0.997
Cu_4/C_3N_5	0.51	1.49	0.26	20.41	021	945.16	223.6	0.996

References

1 P. Kumar, E. Vahidzadeh, U. K. Thakur, P. Kar, K. M. Alam, A. Goswami, N. Mahdi, K. Cui, G. M. Bernard, V. K. Michaelis, K. Shankar. *J. Am. Chem. Soc*. 2019, **141**, 5415-5436.

2 T. Liu, G. Yang, W. Wang, C. Wang, M. Wang, X. Sun, P. Xu, J. Zhang. *Environ. Res*. 2020, **188**, 109741.

3 J. Yang, H. Qi, A. Li, X. Liu, X. Yang, S. Zhang, Q. Zhao, Q. Jiang, Y. Su, L. Zhang. *J. Am. Chem. Soc*. 2022, **144**, 12062-12071.

4 W. Maneeprakorn, M. A. Malik, P. O'Brien. *J. Am. Chem. Soc*. 2010, **6**, 1780-1781.

5 J. Wang, T. Heil, B. Zhu, C.-W. Tung, J. Yu, H. M. Chen, M. Antonietti, S. Cao. *ACS nano* 2020, **14**, 8584-8593.

6 Q. Wang, K. Liu, J. Fu, C. Cai, H. Li, Y. Long, S. Chen, B. Liu, H. Li, W. Li. *Angew. Chem. Int. Ed.* 2021, **60**, 25241-25245.

7 M. Zhang, Y. Mao, X. Bao, G. Zhai, D. Xiao, D. Liu, P. Wang, H. Cheng, Y. Liu, Z. Zheng. *Angew. Chem. Int. Ed*. 2023, **62**, e202302919.

8 Y. Yin, W. Jing, F. Wang, Y. Liu, L. Guo. *Carbon*. 2023, **214**, 118317.

9 W. Wang, S. Song, P. Wang, M. He, Z. Fang, X. Yuan, H. Li, C. Li, X. Wang,Y. Wei. *ACS Catal*. 2023, **13**, 4597-4610.

10 H. Shi, H. Wang, Y. Zhou, J. Li, P. Zhai, X. Li, G. G. Gurzadyan, J. Hou, H. Yang, X. Guo. *Angew. Chem. Int. Ed*. 2021, **61**, e202208904.

11 H. Yu, C. Sun, Y. Xuan, K. Zhang, K. Chang. *Chem. Eng. J*. 2022, **430**, 132940.

12 D. Zhao, Y. Xuan, K. Zhang,X. Liu. *ChemSusChem*. 2021, **14**, 3293-3302.

13 M. Jiang, K. Huang, J. Liu, D. Wang, Y. Wang, X. Wang, Z. Li, X. Wang, Z. Geng, X. Hou, S. Feng. *Chem*. 2020, **6**, 2335-2346.

14 G. Wang, C. He, R. Huang, J. Mao, D. Wang, Y. Li. *J. Am. Chem. Soc.* 2020, **142**, 19339-19345.

15 E. T. Cui, Y. L. Lu, J. Z. Jiang, Arramel, D. S. Wang, T. Y. Zhai, *Chinese J. Catal*. 2024. **59**, 126-136